

Adsorbing trees in two dimensions: A Monte Carlo study

S. You¹ and E. J. Janse van Rensburg²

¹*Department of Physics and Astronomy, York University, Toronto, Ontario, Canada M3J 1P3*

²*Department of Mathematics and Statistics, York University, Toronto, Ontario, Canada M3J 1P3*

(Received 8 February 2001; published 17 September 2001)

Branched polymers interacting with an impenetrable wall can be modeled by lattice trees confined to a half space with a fugacity κ conjugate to the number of visits the tree makes in the wall. We adapt a cut-and-paste algorithm for lattice trees with an umbrella-style implementation to sample trees interacting with an impenetrable wall over a wide range of values for κ . We report results about the thermodynamic and metric properties of the trees, and estimate the location of the adsorption transition κ_c^+ and crossover exponent ϕ .

DOI: 10.1103/PhysRevE.64.046101

PACS number(s): 64.60.Fr, 64.90.+b, 02.70.Rr

I. INTRODUCTION

A polymer in dilute solution can adsorb onto a solid wall if the interaction between the polymer and molecules in the wall exceeds the conformational entropy associated with the polymer in bulk solution. This adsorption phenomenon is a phase transition, which is geometric in nature: The three dimensional extent of the polymer is reduced to a more or less two dimensional nature in the adsorbed phase.

In this paper, we reconsider a lattice tree model of branched polymer adsorption onto a solid wall in two dimensions (2D). The adsorption transitions in models of branched polymers have been reviewed by De'Bell and Lookman [1], where the values of several critical exponents associated with the model were reported. Further work includes a transfer matrix study by de Queiroz [2] and exact (but not rigorous) results in three dimensions by Janssen and Lyssy [3]. Earlier Monte Carlo studies of a model of branched polymers near a wall were done by Lam and Binder [4]. Our approach is also a Monte Carlo simulation, but using a cut-and-paste algorithm for lattice trees [5] on the square lattice. Our motivation for the simulation is to find good numerical estimates of both the critical point and the critical exponents associated with the adsorption transition. Of particular importance is the crossover exponent ϕ ; a suggestion of hyperuniversality [2] for branched polymer adsorption indicates that $\phi = 1/2$, although the real test for this prediction will only come with estimates of ϕ in higher dimensions.

A tree is called attached if it has at least one vertex with z coordinate equal to $-1, 0$, or 1 . A tree confined to the half space $z \geq 0$ is a positive tree. A common model for a branched polymer in the vicinity of a solid wall is a positive attached tree. A visit is a vertex in a lattice tree with z coordinate equal to zero. The fundamental quantity in this model is $t_n^+(v)$, which is the number of positive attached trees with n edges and v visits. Trees are weighted by the number of visits they have: a tree with v visits will have weight $e^{\kappa v}$, where κ is a fugacity conjugate to v . The partition function for positive attached trees is

$$Z_n^+(\kappa) = \sum_{v \geq 0} t_n^+(v) e^{\kappa v}. \quad (1)$$

The limiting free energy of this model is the thermodynamic limit of $\ln Z_n^+(\kappa)$ per edge; this is known to exist [6], and is defined by

$$\mathcal{F}^+(\kappa) = \lim_{n \rightarrow \infty} \frac{1}{n} \ln Z_n^+(\kappa) \quad \text{for all } \kappa < \infty. \quad (2)$$

Moreover, $\mathcal{F}^+(\kappa)$ is a convex function, and is nondecreasing, continuous, and differentiable almost everywhere [6]. It is also known that the limiting free energy $\mathcal{F}^+(\kappa)$ is independent of κ for all $\kappa \leq 0$ [$\mathcal{F}^+(\kappa) = \ln \lambda_2$ where λ_2 is the growth constant of lattice trees in two dimensions]. If $\kappa > 0$, then it has been shown that $\max\{\ln \lambda_{2,\kappa}\} \leq \mathcal{F}^+(\kappa) \leq \ln \lambda_2 + \kappa$ for $\kappa > 0$. These bounds imply the existence of a nonanalyticity at a critical value κ_c^+ in the free energy of positive trees, and this corresponds to the adsorption transition of a branched polymer on a solid wall. The critical value of the fugacity may be defined by

$$\kappa_c^+ = \sup\{\kappa | \mathcal{F}^+(\kappa) = \ln \lambda_2\} \quad (3)$$

in two dimensions and it is known that $\kappa_c^+ > 0$ [6]. The density of visits is defined by $\langle v/n \rangle = (1/n) \partial \ln Z_n^+(\kappa) / \partial \kappa$ where $\langle v/n \rangle \rightarrow \langle V \rangle = \partial \mathcal{F}^+ / \partial \kappa$ as $n \rightarrow \infty$. κ_c^+ is also that value of the fugacity where the density of visits $\langle V \rangle$ becomes non-zero: $\langle V \rangle = 0$ if $\kappa < \kappa_c^+$ and $\langle V \rangle > 0$ if $\kappa > \kappa_c^+$. By the convexity of the limiting free energy, $\langle V \rangle = \partial \mathcal{F}^+(\kappa) / \partial \kappa$, and this exists for almost every value of κ .

An umbrella sampling implementation of the cut-and-paste algorithm was used over a wide range of κ . This type of implementation was also used in the sampling of collapsing trees in a self-interacting model of lattice trees [5], and similarly in the simulation of collapsing lattice animals [8]. We shall collect thermodynamic data and metric data on adsorbing positive attached trees in this simulation in order to locate the adsorption transition at a critical value of κ (κ_c^+) and to find numerical estimates of critical exponents associated with the transition.

The metric exponent ν describes scaling of quantities with dimensions of length, and, in particular, one would expect that

$$\langle R_n(\kappa) \rangle \sim n^{\nu(\kappa)} \quad (4)$$

where $R_n(\kappa)$ is a metric quantity, and where we now note that ν may depend on κ . It is known that $\nu(0) \approx 0.64$ in two dimensions, and, in fact, one would expect that $\nu(\kappa) \approx 0.64$ for all $\kappa < \kappa_c^+$ in two dimensions. On the other hand, since the tree has a nonzero density of visits in the adsorbed phase, its span along the adsorbing wall will be $O(n)$ in two dimensions so that $\nu(\kappa) = 1$ if $\kappa > \kappa_c^+$ in two dimensions.

The branch exponent ρ measures an intrinsic length in a model of lattice trees. It is defined by

$$\langle P_n(\kappa) \rangle \sim n^{\rho(\kappa)}, \quad (5)$$

where $P_n(\kappa)$ is the length of the longest path in a tree [7]. If a lattice tree is cut into two subtrees by deleting an edge, then the smaller of the subtrees is called a branch. It is believed that the mean branch size scales with the exponent ρ as well: $\langle B_n(\kappa) \rangle \sim n^{\rho(\kappa)}$ [7]. The value of ρ for trees in two dimensions is estimated to be about $3/4$, and one should expect this value as well for positive trees in the desorbed phase, $\rho(\kappa) \approx 3/4$ if $\kappa < \kappa_c^+$. In the adsorbed phase the span of the tree along the adsorbing wall should grow linearly with the size of the tree, and so we expect here that $\rho(\kappa) = 1$ if $\kappa > \kappa_c^+$.

Thermodynamic data are equally important in analyzing the properties of the adsorbing lattice tree. The starting point is the finite size free energy per monomer: $F_n^+(\kappa) = (1/n) \ln Z_n(\kappa)$. The specific heat is defined by $C_n^+(\kappa) = d^2 F_n^+(\kappa) / d\kappa^2$ and this is equal to $(\langle v^2 \rangle - \langle v \rangle^2) / n$. These are analytic functions for finite values of n , but as $n \rightarrow \infty$, $F_n^+(\kappa) \rightarrow \mathcal{F}^+(\kappa)$, the limiting free energy, which we know to be a nonanalytic function. The standard finite size scaling ansatz for $F_n^+(\kappa)$ is [9,10]

$$F_n^+(\kappa) \sim \tau^{2-\alpha} f(n\tau^{1/\phi}) \quad \text{where } \tau = (\kappa - \kappa_c) / \kappa_c. \quad (6)$$

where ϕ is a crossover exponent that describes the crossover behavior of $F_n^+(\kappa)$ to $\mathcal{F}^+(\kappa)$ as $n \rightarrow \infty$. α is the specific heat exponent, and it describes the nonanalyticity in the limiting free energy. The function $f(x)$ is a universal scaling function, and $f(x) \rightarrow \text{const}$ as $x \rightarrow \infty$. The singular part of the limiting free energy behaves as $\mathcal{F}^+(\kappa) \sim \tau^{2-\alpha}$. If we define $g(x) = x^{\phi(2-\alpha)} f(x)$, then we obtain

$$F_n^+(\kappa) \sim n^{\phi(2-\alpha)} g(n^{\phi} \tau), \quad \tau \geq 0. \quad (7)$$

Since we know that $F_n^+(\kappa) = (1/n) \ln Z_n^+(\kappa)$, this shows that $2 - \alpha = 1/\phi$, the standard hyperscaling relation that relates the specific heat exponent to the crossover exponent.

Since the singular part of the limiting free energy is assumed to behave as $\tau^{2-\alpha}$, the specific heat should have a singularity of the form

$$C(\kappa) \sim \tau^{-\alpha}, \quad \tau \geq 0. \quad (8)$$

It is known that $\mathcal{F}^+(\kappa) = \ln \lambda_2$ if $\tau < 0$ and so $C(\kappa) = 0$ if $\tau < 0$. If n is finite, then we can compute from Eq. (7) that

$$C_n(\kappa) \sim n^{\phi\alpha} g''(n^{\phi} \tau), \quad \tau \geq 0. \quad (9)$$

If $\kappa < \kappa_c^+$, then $C_n(\kappa) \rightarrow 0$ with increasing n , while, if $\kappa > \kappa_c^+$, $C_n(\kappa)$ should either diverge (if $\phi\alpha > 0$), or approach a limiting curve, such as a cusp (if $\phi\alpha = 0$). If it increases with increasing n , then the curves $C_n(\kappa)$ should intersect at the critical point, and this will give us one way of finding the critical value of κ . In this model it is believed that $\phi = 1/2$ (and thus $\alpha = 0$) so that the specific heat will have a cusp singularity at the critical point. Numerically, this is more difficult to analyze than a divergent specific heat, and we shall rely on the intersections between the curves $C_n(\kappa)$ to locate the critical point.

II. MARKOV CHAIN SAMPLING

The cut-and-paste algorithm for lattice trees performs poorly in the adsorbed phase of the lattice trees (that is, for large values of κ). Since it is a Metropolis algorithm, it operates by sampling along a Markov chain in the state space of positive trees. A typical simulation would have long excursions in some relatively small regions of state space, with the result that there are systematic errors in the averages computed by a simulation. This is referred to as a *quasi-ergodic problem*, and in this case it is caused by the inability of the algorithm to make large changes to the tree (these would break many visits, and so are unfavorable). By lowering the value of κ in a simulation, this problem can be alleviated. One such technique (which effectively lowers the strength of the interaction in the simulation) is called umbrella sampling [11], and this was also implemented in studies of collapsing trees [5].

A Metropolis algorithm sampling from a canonical Boltzmann distribution can be turned into an umbrella sampling algorithm by simply replacing the Boltzmann distribution by an arbitrary distribution π . Canonical averages can then be obtained by relying on the following importance sampling identity:

$$\begin{aligned} \langle Q(\kappa) \rangle &= \frac{\sum_{j=1}^{t_n^+} Q(j) e^{v(j)\kappa}}{\sum_{j=1}^{t_n^+} e^{v(j)\kappa}} \\ &= \frac{\sum_{j=1}^{t_n^+} Q(j) e^{v(j)\kappa} \pi_j / \pi_j}{\sum_{j=1}^{t_n^+} e^{v(j)\kappa} \pi_j / \pi_j} \\ &= \frac{\langle Q e^{v\kappa} / \pi \rangle_{\pi}}{\langle e^{v\kappa} / \pi \rangle_{\pi}}, \end{aligned} \quad (10)$$

where $Q(j)$ is the value of the property Q for the j th tree, $v(j)$ is the number of visits in the j th tree, and the subscript π denotes expectation with respect to the distribution π .

It is important to note that relation (10) is true for any probability distribution π . Sampling from π can be carried out using a Metropolis rejection scheme with a suitable selection of trial moves. If one chooses π to overlap the Boltzmann distributions at those values of κ of interest to us, and distributions at values of κ where the Markov chain is mo-

TABLE I. The number of data collected and their step sizes.

n	Number of data collected	Step size
25	50 000	250
50	50 000	1 000
75	50 000	3 000
100	250 000	4 000
150	250 000	6 000
200	1 000 000	8 000
300	1 000 000	15 000
400	1 000 000	32 000
500	1 000 000	40 000

bile, then a more efficient sampling process is found, even for those values of κ where Boltzmann sampling is difficult.

There is no obvious criterion for the best choice of the umbrella distribution π . An often used distribution is a linear combination of the Boltzmann distributions of interest, with a ‘‘flat histogram criterion’’ [5]: each Boltzmann distribution must make about the same contribution to the umbrella distribution. The flatness criterion is implemented by repeating simulations, using data from each simulation to improve the umbrella for the next until a histogram that is sufficiently flat is obtained.

In our simulations we collected data primarily on the number of visits (v), the mean square radius of gyration (R_n^2), the mean span (S_n), the mean end-to-end distance of the longest path (E_n), the mean longest path (P_n), and the mean branch size (B_n). Runs were performed on trees of sizes from $n = 25$ to 500 edges. The step size in Table I is the number of attempted elementary moves between collected data points. Increasing this reduces autocorrelations in the data stream. For larger trees very large step sizes were necessary to reduce autocorrelations (which were computed and factored into the statistical analysis of our confidence intervals).

Our immediate motivations are to obtain high quality data for the estimation of the crossover exponent ϕ and the critical value of κ , κ_c^+ . Umbrellas were generated using histogram uniformization by repeated simulations as necessary. The umbrellas were checked by performing Monte Carlo runs with Boltzmann distributions to compare the results with umbrella sampling results.

III. RESULTS

Our data show an increase in the mean square radius of gyration as κ increases. This effect is best illustrated by considering ratios of $R_n^2/n^{2\nu}$. In particular, if $R_n^2(\kappa)$ is the mean square radius of gyration at κ in trees with n edges, then we should expect that

$$\frac{R_n^2(\kappa)}{n^{2\nu}} \sim \begin{cases} \text{const} & \text{if } \kappa \leq \kappa_c^+ \\ \infty & \text{if } \kappa > \kappa_c^+ \end{cases} \text{ as } n \rightarrow \infty. \quad (11)$$

If we assume that $R_n^2(\kappa)/n^{2\nu}$ decreases to a constant for $\kappa \leq \kappa_c^+$, then these curves should intersect each other at κ_c^+ , when plotted against κ .

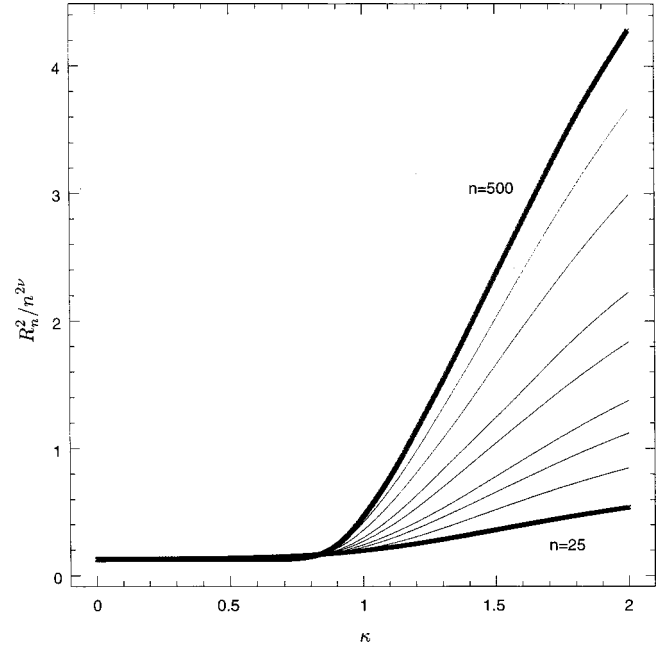


FIG. 1. The ratios of the mean square radius of gyration for trees of size n to $n^{2\nu}$, $R_n^2/n^{2\nu}$, for $n = 25$ to 500.

We plot the ratio $R_n^2/n^{2\nu}$ against κ in Fig. 1. These curves approach the value 0.125 if $\kappa=0$, and, if we assume the model $R_n^2 = An^{2\nu}(1 + bn^{-\Delta})$, where $\Delta = 0.65$ [12] is the first or effective confluent correction, then a least squares fit at $\kappa=0$ gives $\nu = 0.6425 \pm 0.0002$ as the metric exponent for lattice trees.

The exponent ν can also be obtained by analyzing data obtained from the end-to-end distance of the longest path, E_n , and the mean span S_n of the tree. On the other hand, the results from these analyses are conditioned on the assumed model. A different model may give a different best estimate for ν . Should this be the case, then it may be assumed that this is indicative of a systematic error in the estimates of the exponent ν . We therefore tried a different, but related, model to see the effect of the choice of model on the estimates for ν . A two parameter linear model (where the confluent correction is ignored) gave a slightly different estimate for ν . We take the absolute difference in two results from the two models as a measure of the size of a possible systematic error. Our estimates for ν are listed in Table II.

The data collected for the mean path P_n and the mean branch size B_n were analyzed in a fashion similar to ν above and the results are listed in Table III. The results in Table II were all obtained by a least square analysis, all of them with

TABLE II. Metric exponent ν at $\kappa=0$.

Quantity	ν with $\Delta=0.65$	ν with two-parameter fit	Systematic error
R_n^2	0.64 248(16)	0.6351(27)	0.0074
E_n	0.64 000(60)	0.6481(26)	0.0081
S_n	0.63 780(39)	0.6673(52)	0.0295

TABLE III. Branch exponent ρ at $\kappa=0$.

Quantity	ρ with $\Delta=0.65$	ρ with two-parameter fit	Systematic error
B_n	0.74 212(54)	0.7294(20)	0.0127
P_n	0.73 682(47)	0.73819(62)	0.0004

a χ^2 statistic acceptable at the 95% level. We find our best estimate by taking the average of these:

$$\nu = 0.645 \pm 0.007 \pm 0.020,$$

where we first state a 95% statistical confidence interval (we take the largest such confidence interval in Table II, and then round it up), and then an estimated systematic error (which is one-half the maximum difference between estimates in Table II).

The best estimate for ρ can be similarly obtained. We found

$$\rho = 0.737 \pm 0.002 \pm 0.007.$$

If we present these best estimates with error bars as the sums of statistical and systematic errors, then we have

$$\nu = 0.645 \pm 0.030m, \quad \rho = 0.737 \pm 0.010.$$

They are remarkably close to the values for lattice trees obtained previously in 2D [12], which are $\nu = 0.642 \pm 0.010$ and $\rho = 0.738 \pm 0.010$.

From the points of intersection in Fig. 2, we can estimate the value of κ_c^+ by drawing the smallest rectangle around the points of intersection between the various curves. The analysis for three other quantities (the end-to-end distance of the

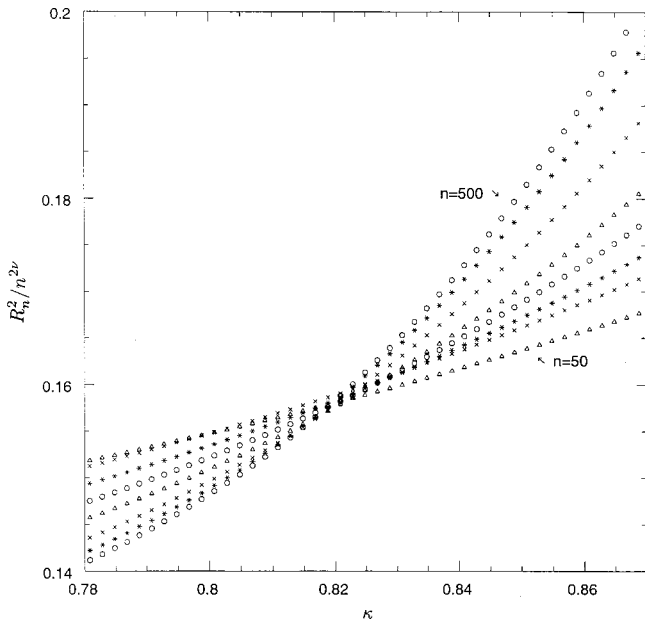


FIG. 2. The ratios of the mean square radius of gyration for trees of size n to $n^{2\nu}$, $R_n^2/n^{2\nu}$, for $n=50$ to 500 focused on the intersections of the curves.

TABLE IV. Estimates of κ_c^+ from the ratios of the listed quantities to n^ν or n^ρ , where n_{\min} is the size of the smallest tree included in the analysis.

Quantity	n_{\min}	κ_c^+
R_n^2	50	0.821(17)
E_n	75	0.807(15)
B_n	50	0.821(28)
P_n	75	0.779(28)

longest path in the tree E_n , the mean branch size B_n , and the longest path in the tree P_n) follows the same general lines as for the mean square radius of gyration (R_n^2). In other words, we plot $R_n^2(\kappa)/n^{2\nu}$, E_n/n^ν , B_n/n^ρ , and P_n/n^ρ against κ , and look for the intersections of the curves. Here we set $\nu = 0.642$ and $\rho = 0.738$, which are the best estimates for the free trees in two dimensions [12]. The error bars are obtained by taking one-half the maximum difference between the intersections. We also tried to confirm these error bars by using two other different approaches in determining them. In the first instance we took the average of the intersections while discarding outlier points; this gives error bars of size 50% to 100% of those stated in Table IV. In the second instance we looked at the envelope of the set of intersecting curves. We determined the critical point at its narrowest part (its waist), and a confidence interval by searching for that interval with end points at values of κ where the envelope has increased to a size that is 1.5 times its narrowest size. This method gave error bars of size 20% to 30% of those in Table IV. The consistency in the outcome of these three methods supports the estimates made in Table IV, and may even indicate that our stated error bars are somewhat conservative. The mean span S_n does not show clear intersections of the curves and is

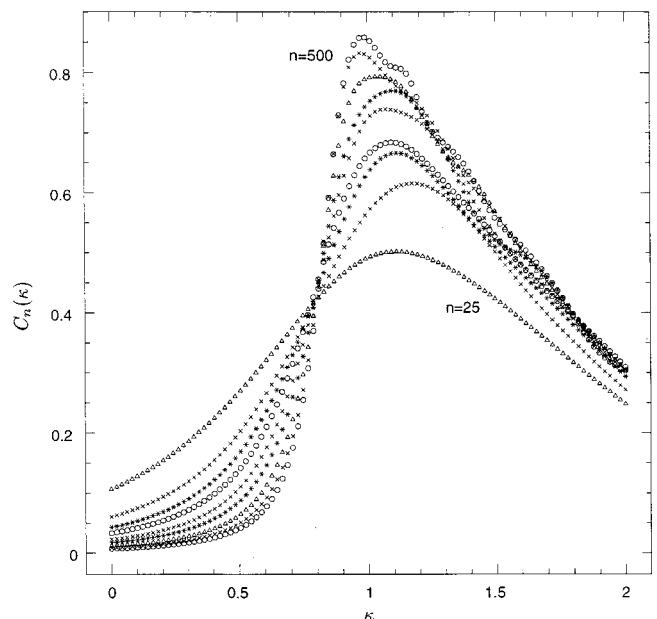


FIG. 3. Specific heat for trees of $n=25$ to $n=500$.

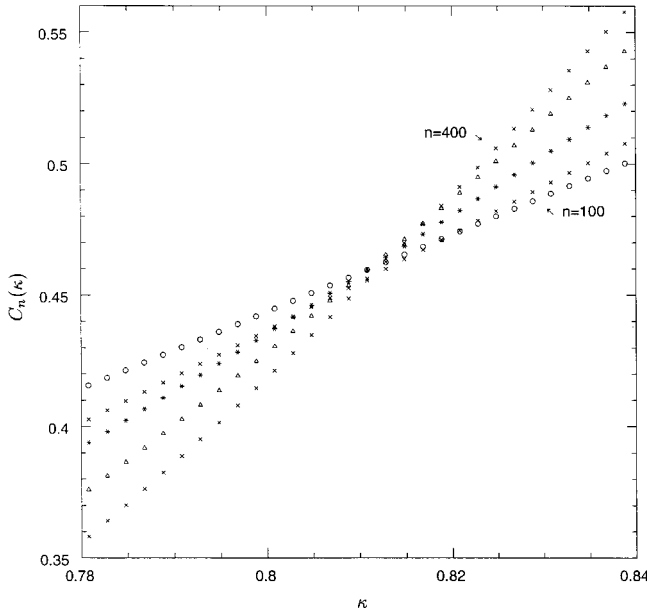


FIG. 4. Specific heat for trees from $n=100$ to $n=400$ focused on the intersections of the curves.

excluded for this estimate. The average value of κ_c^+ obtained from Table IV is then

$$\kappa_c^+ = 0.81 \pm 0.03, \quad (12)$$

where the error bar is one-half the absolute difference between the smallest and largest estimate, rounded up.

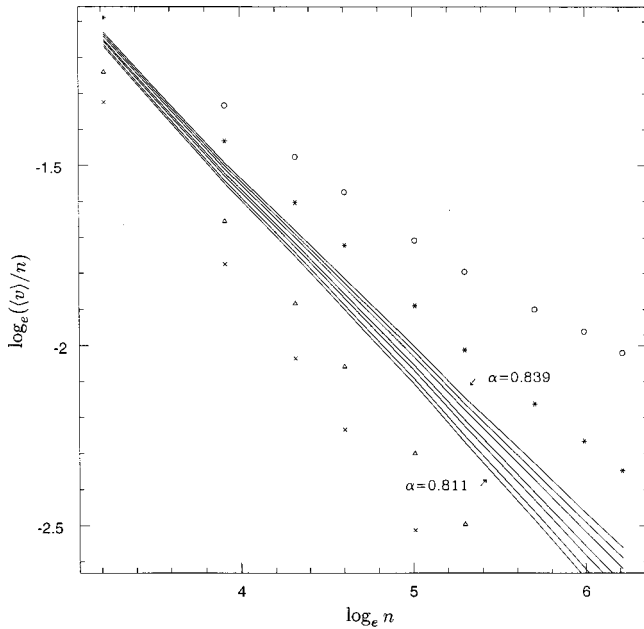


FIG. 5. Log-log plots of the average energy per edge, $\langle v \rangle/n$, vs tree size n for different values of κ . Approximate straight lines are observed at $0.811 \leq \kappa \leq 0.839$ (solid lines), which are compared with other plots with different values of κ (\times , $\kappa=0.699$; \triangle , $\kappa=0.759$; $*$, $\kappa=0.869$, and \circ , $\kappa=0.919$). As we increase κ , the slopes of the lines increase.

TABLE V. Estimates of ϕ from $\ln(\langle v \rangle/n)$ plotted against $\ln(n)$ with several values of κ .

κ	ϕ
0.811	0.4703(70)
0.815	0.4784(65)
0.821	0.4901(63)
0.825	0.4979(69)
0.831	0.5098(82)
0.835	0.5178(97)
0.839	0.526(11)

The specific heat data obtained in our simulations were similarly analyzed (see Figs. 3 and 4). It appears again that the critical value of κ can be obtained by looking at intersections between curves, and our analysis gives

$$\kappa_c^+ = 0.811 \pm 0.010. \quad (13)$$

We omitted the results for the first three small trees ($n=25, 50$, and 75) due to strong correction to scaling effects, and we have also omitted the results for the largest tree since the data at $n=500$ are so close to the data obtained from $n=400$ that we could not determine an intersection between their curves accurately.

The critical values of κ_c^+ can also be determined from the expected behavior of the energy $\langle v \rangle$ at κ_c^+ . From Eq. (7), we have

$$\frac{\partial F_n^+}{\partial \tau} \sim n^{\phi - \phi(2-\alpha)} g'(n^{\phi} \tau) \sim n^{\phi-1},$$

since $\phi(2-\alpha)=1$ by the hyperscaling relation. Thus,

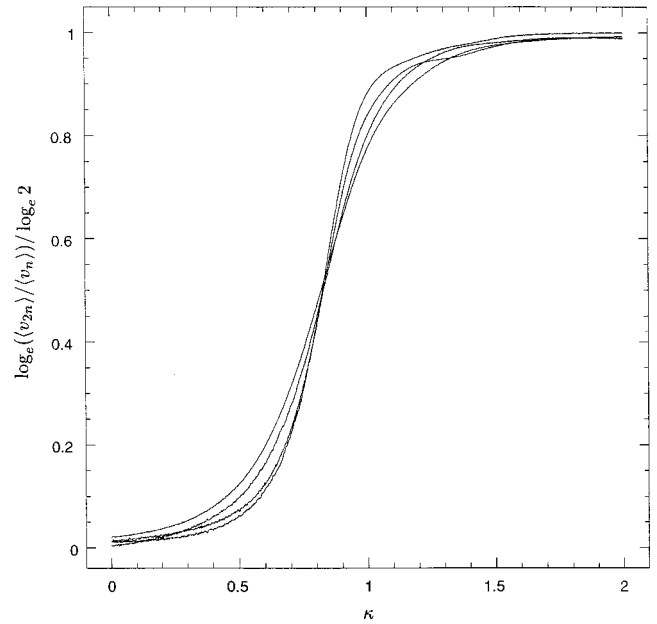


FIG. 6. Plots of energy ratios $\log_e(\langle v_{2n} \rangle / \langle v_n \rangle) / \log_e(2)$ against κ for $n=75, 100, 150$, and 200 . The intersection point defines both critical value κ_c^+ and the crossover exponent ϕ .

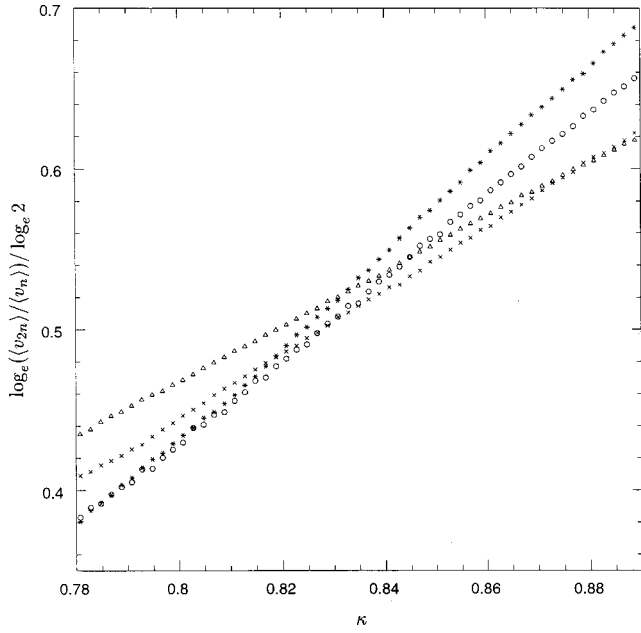


FIG. 7. Plots of energy ratios $\log_e(\langle v_{2n} \rangle / \langle v_n \rangle) / \log_e(2)$ against κ for $n = 75, 100, 150,$ and 200 focused on intersection points.

$$n \frac{\partial F_n^+}{\partial \tau} = \langle v \rangle \sim n^\phi,$$

where ϕ is a crossover exponent. For $\kappa > \kappa_c^+$, the energy of a very big tree becomes extensive ($\sim n$), while in the region for $\kappa < \kappa_c^+$ $\langle v \rangle$ is constant, i.e., it does not increase with increasing n . Therefore, a log-log plot of the results for $\langle v \rangle / n$ versus n for different values of κ will be a straight line at κ_c^+ with a negative slope equal to $\phi - 1$ (Fig. 5). Approximate straight lines occur in the range $0.811 \leq \kappa \leq 0.839$ (Table V). The value of ϕ estimated from the center solid line in Fig. 5 is

$$\phi = 0.50 \pm 0.03, \tag{14}$$

where the error bar is one-half the difference between the largest and smallest estimates.

As a last check on the results above we also found κ_c^+ and ϕ as follows. At κ_c^+ one expects (if corrections to scaling are ignored) $\langle v_{2n} \rangle / \langle v_n \rangle = 2^\phi$, which is a constant. These ratios for $n = 75, 100, 150,$ and 200 can be plotted as a function of

TABLE VI. Estimate of κ_c^+ and ϕ from the individual intersections among the curves of $\ln(\langle v_{2n} \rangle / \langle v_n \rangle) / \ln 2$ versus $\ln(n)$. The intersection between the ratios for $n = 150$ and 200 is excluded for this analysis.

κ_c^+	ϕ
0.873	0.592
0.845	0.545
0.833	0.524
0.827	0.498
0.819	0.483

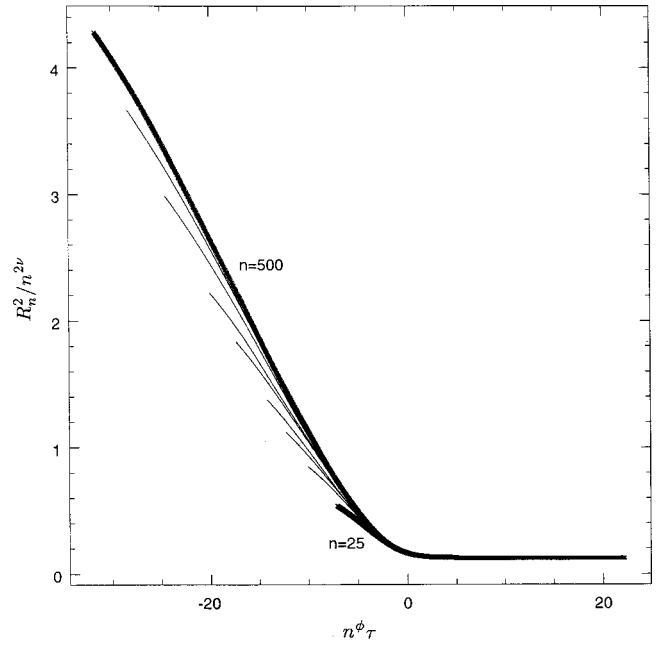


FIG. 8. $R_{2n}^2(\kappa) / n^{2\nu}$ against $n^\phi \tau$ with $\kappa = 0.81$ and $\phi = 0.50$.

κ , where the intersection point of the lines (at which the above energy ratios become constant) defines both κ_c^+ and ϕ (see Fig. 6). The results for $n = 25$ and 50 are omitted due to strong correction to scaling effects. In Fig. 7, the intersections of these lines are focused, and all possible individual intersections among four lines (except those between $n = 150$ and 200 since they show many intersections in a wide range of κ) are considered separately to find each location κ_c^+ and the value of the ratio at this location, ϕ (Table VI). The first estimate of $\kappa_c^+ = 0.873$ is outside the error bars obtained in Eqs. (12) and (13), and we ignore it in our analysis.

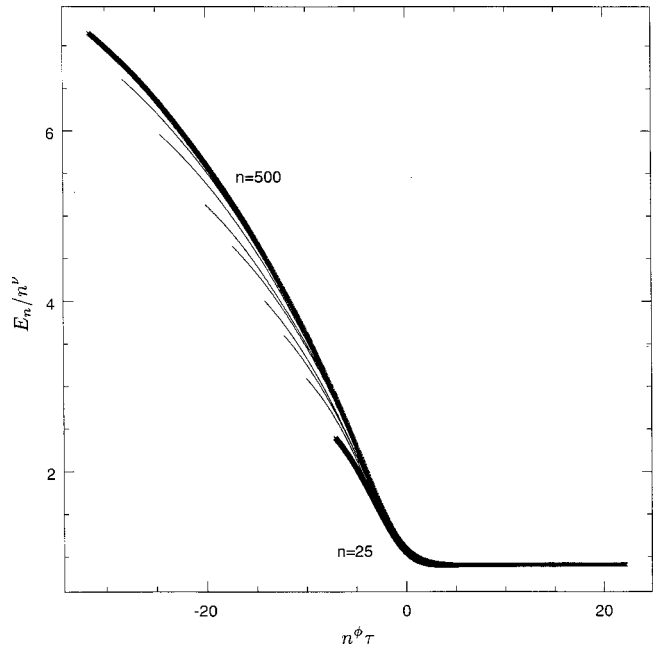


FIG. 9. $E_n(\kappa) / n^\nu$ against $n^\phi \tau$ with $\kappa = 0.81$ and $\phi = 0.50$.

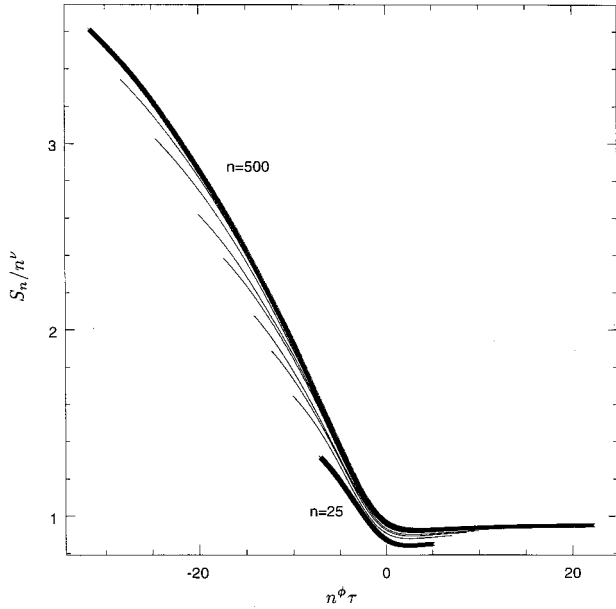


FIG. 10. $S_n(\kappa)/n^\nu$ against $n^\phi\tau$ with $\kappa=0.81$ and $\phi=0.50$.

The remaining data points are consistent with our other estimates. If these are averaged, and errors bars are computed by taking one-half the distance between the largest and smallest, then $\kappa_c^+ = 0.83 \pm 0.02$ and $\phi = 0.51 \pm 0.04$, not inconsistent with the previously obtained results.

The scaling assumption for the mean square radius of gyration is $R_n^2(\kappa) \sim n^{2\nu} h_1(n^\phi\tau)$ where $h_1(x)$ is a suitable scaling function. It is not unreasonable to expect that a plot of $R_n^2(\kappa)$ against $n^\phi\tau$ will reveal the shape of the scaling function. If the ratios $R_{2n}^2(\kappa)/n^{2\nu}$ are taken, then

$$\frac{R_{2n}^2(\kappa)}{n^{2\nu}} \sim h_1(n^\phi\tau). \quad (15)$$

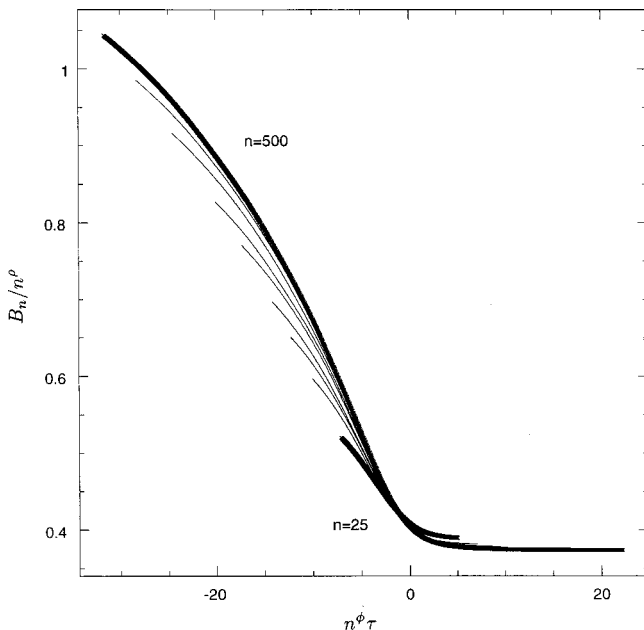


FIG. 11. $B_n(\kappa)/n^\rho$ against $n^\phi\tau$ with $\kappa=0.81$ and $\phi=0.50$.

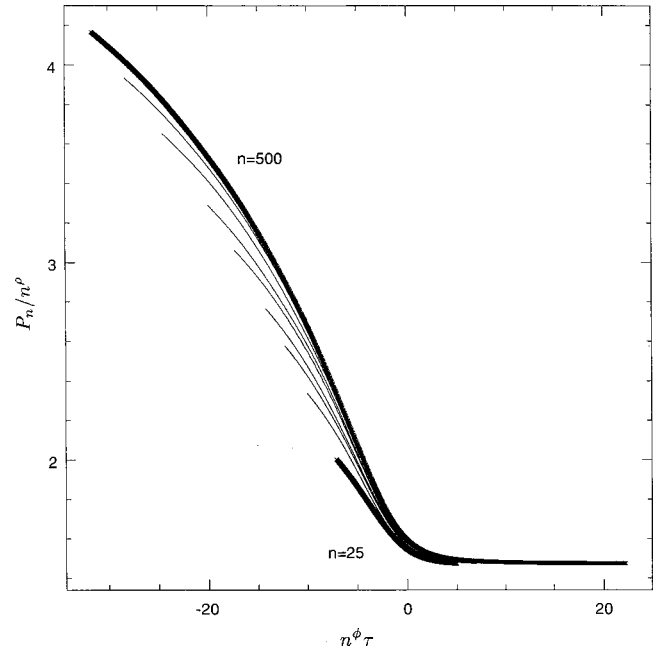


FIG. 12. $P_n(\kappa)/n^\rho$ against $n^\phi\tau$ with $\kappa=0.81$ and $\phi=0.50$.

Since this ratio is independent of n , one can use this as another check on the estimates of ϕ and κ_c^+ . We plot it with various values of ϕ and κ_c^+ until the data collapse to a single curve. Our attempts with the best estimates $\phi=0.50$ and $\kappa_c^+=0.81$ are illustrated in Figs. 8–12.

We next analyze the metric data to estimate the exponents ν and ρ as functions of κ (see Figs. 13–15). These exponents should change abruptly around κ_c^+ , and indicate that the thermodynamic phase transition is accompanied by a transition in metric properties consistent with adsorption. The values of ν and ρ in the phase with large κ are consistent with it being a primarily linear object extending along the adsorbing line.

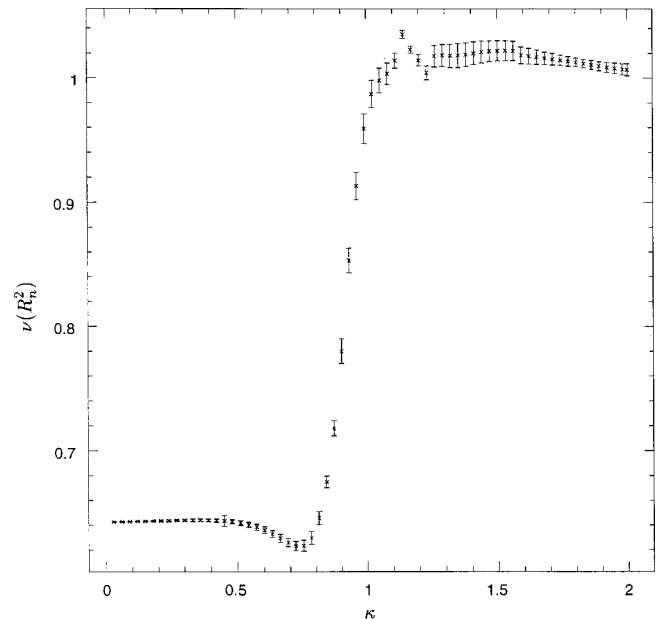
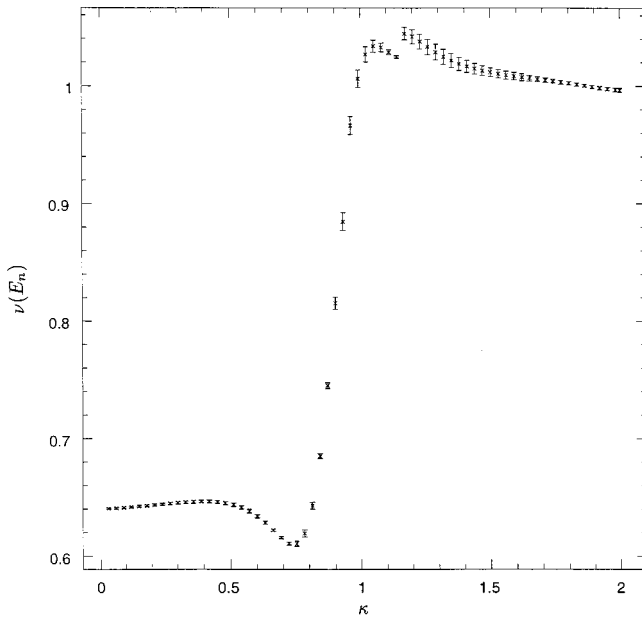


FIG. 13. The metric exponent ν estimated from $R_n^2(\kappa)$ against κ .

FIG. 14. The metric exponent ν estimated from $E_n(\kappa)$ against κ .

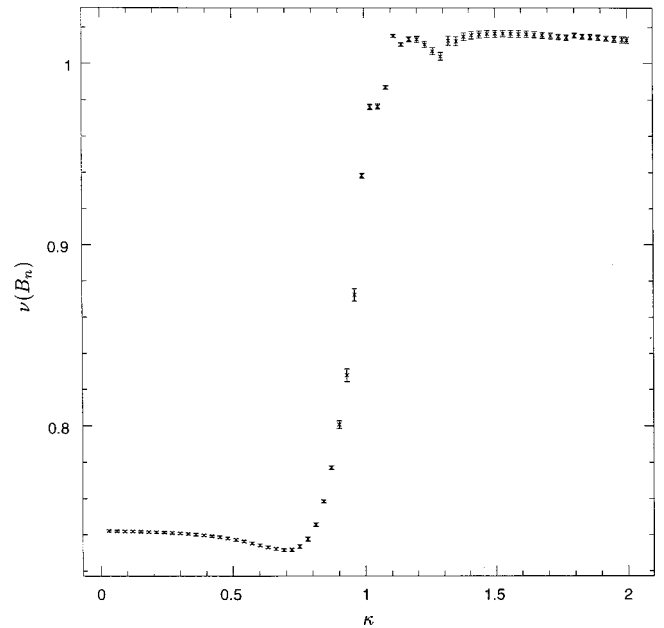
IV. CONCLUSION

We have performed extensive simulations of lattice trees interacting with a solid wall in two dimensions. The cut-and-paste algorithm for trees has been adapted via umbrella sampling to deal with quasiergodic problems, and it successfully sampled trees over a wide range of values of κ .

The crossover exponent and critical value of κ have been computed in several ways. All our results agree within their error bars. Our best estimates for ϕ and κ_c^+ are found from Eqs. (14), (12), and (13). These are

$$\phi = 0.50 \pm 0.03, \quad \kappa_c^+ = 0.81 \pm 0.03$$

for adsorbing lattice trees. From an exact study of the Ising model in an imaginary field in $d=1$, the result $\phi=0.5$ is obtained for lattice tree adsorption in $d=3$ [3,13]. In two dimensions the crossover exponent for adsorbing branched polymers is thought to be equal to $1/2$, consistent with our result above. An approach using the transfer matrix gives the

FIG. 15. The branch exponent ρ estimated from $B_n(\kappa)$ against κ .

estimate $\phi = 0.505 \pm 0.015$ (de Queiroz [2]). These results are consistent with the notion of hyperuniversality in adsorbing branched polymers [3]; that is, $\phi = 1/2$ in every dimension for adsorbing branched polymers.

It is also the case that values close to $1/2$ have been obtained for the crossover exponent of adsorbing linear polymers. Numerical data in three dimensions suggest that $\phi \approx 1/2$ [14], while renormalization group calculations and series estimates gave larger values for ϕ [15,16]. In two dimensions the result that $\phi = 1/2$ has been obtained using a variety of techniques [17–19]; see also [20] and [21] for more details.

ACKNOWLEDGMENT

E.J.J.vR. is supported by an operating grant from NSERC (Canada).

-
- [1] K. De'Bell and T. Lookman, *Rev. Mod. Phys.* **65**, 87 (1992).
 - [2] S. L. A. de Queiroz, *J. Phys. A* **28**, 6315 (1995).
 - [3] H. K. Janssen and A. Lyssy, *Phys. Rev. A* **44**, 1390 (1994).
 - [4] P. M. Lam and K. Binder, *J. Phys. A* **21**, L405 (1988).
 - [5] N. Madras and E. J. Janse van Rensburg, *J. Stat. Phys.* **86**, 1 (1997).
 - [6] E. J. Janse van Rensburg and S. You, *J. Phys. A* **31**, 8635 (1998).
 - [7] E. J. Janse van Rensburg and N. Madras, *J. Phys. A* **25**, 303 (1992).
 - [8] E. J. Janse van Rensburg, E. Orlandini, and M. C. Tesi, *J. Phys. A* **32**, 1567 (1999).
 - [9] I. D. Lawrie and S. Sarlbach, in *Phase Transitions and Critical Phenomena*, edited by C. Domb and J. L. Lebowitz (Academic, New York, 1984), Vol. 9, p. 1.
 - [10] A. L. Owczarek, T. Prellberg, and R. Brak, *J. Phys. A* **26**, 4565 (1993).
 - [11] G. M. Torrie and J. P. Valleau, *J. Comput. Phys.* **23**, 187 (1977).
 - [12] S. You and E. J. Janse van Rensburg, *Phys. Rev. E* **58**, 3971 (1998).
 - [13] G. Parisi and S. Sorella, *Phys. Rev. Lett.* **46**, 871 (1981).
 - [14] R. Hegger and P. Grassberger, *J. Phys. A* **27**, 4069 (1994).
 - [15] E. Eisenriegler, *J. Chem. Phys.* **79**, 1052 (1983).

- [16] D. Zhao, T. Lookman, and K. De'Bell, Phys. Rev. A **42**, 4591 (1990).
- [17] M. T. Batchelor and C. M. Yung, Phys. Rev. Lett. **74**, 2026 (1995).
- [18] D. Bennett-Wood and A. L. Owczarek, J. Phys. A **29**, 4755 (1996).
- [19] T. W. Burkhardt and I. Guim, J. Phys. A **24**, L1221 (1991).
- [20] H. Meirovitch and I. Chang, Phys. Rev. E **48**, 1960 (1993).
- [21] C. Vanderzande, in *Lattice Models of Polymers*, edited by P. Goddard and J. Yeomans (Cambridge University Press, Cambridge, 1998).